

Modeling on Shrinkage Stress in Early-Age Concrete Pavements

Zhang Jun¹⁺, Gao Yuan¹, Han Yudong¹, and Wang Qiang¹

Abstract: In this paper, an integrative model for autogenous and drying shrinkage predictions of concrete at early-age is introduced first. Second, a model taking both cement hydration and moisture diffusion into account synchronously is used to calculate the distribution of interior humidity in concrete. Using the two models, the distribution of shrinkage strain in early-age concrete pavements under the condition that the pavement surface suffers to dry is calculated. Afterwards, the shrinkage stress resulted from the nonlinear shrinkage strain is calculated by dividing the shrinkage strain into uniform strain, linear strain and nonlinear strain. The model results show that the gradient of shrinkage strain and stress along the slab depth is obvious under the condition that the slab top suffers to dry. The maximum and minimum shrinkage strain and stress occurs at slab top and bottom respectively. The distribution of shrinkage strain and stress along the pavement depth are nonlinear and the nonlinearity is strong close to the drying face and the rest is weak.

DOI:10.6135/ijprt.org.tw/2013.6(4).250

Key words: Concrete pavement; Model; Shrinkage stress.

Introduction

Concrete shrinks as moisture is lost to the environment or by self-desiccation. As concrete shrinks, a certain amount of tensile stresses will be developed in the structure due to restraints from adjunct materials or connected members. The stresses may exceed the tensile strength and cause concrete to crack. Cracking in concrete members reduces the load capacity of the structure. Moreover, cracks allow water and other chemical agents, such as deicing salt, to go through the cover layer to come into contact with the reinforcements, leading to reinforcement corrosion and rupture in steel reinforced concrete. The magnitude of the shrinkage strain is normally proportional to the amount of moisture lost [1-3]. Generally, there are two manners leading the moisture loss in early-age concrete. As environmental humidity is lower than the humidity inside of concrete, water in concrete evaporates and shrinkage of concrete arises, which is conventionally called drying shrinkage. Another manner of moisture loss is through cement hydration, which causes concrete to shrink also and ordinarily is called autogenous shrinkage. In practice, more water loss may happen at the places where are close to surfaces of concrete elements. Thus, shrinkage gradient should exist in concrete structures and corresponding nonlinear shrinkage stresses should be resulted. However, the effects of shrinkage gradient occurred in concrete structures have not properly been taken into account in the analyses of shrinkage stress in the structures due to the lack of an appropriate model to relate the shrinkage strain and the amount of local moisture loss.

This article focuses on the numerical modelling of the distribution of shrinkage strain and stress in early-age concrete pavement in which the shrinkage gradient is seriously taken into account. In the modelling, an integrative model for autogenous and drying shrinkage prediction of concrete at early-age is introduced first. Second, a model taking both cement hydration and moisture diffusion into account synchronously is used to calculate the

distribution of interior humidity in concrete. Using the models, the distribution of shrinkage strain and stress in early-age concrete pavements under the condition of the pavement suffering to dry is calculated.

Modeling on Moisture Variation Induced Strain

In fresh concrete, all pores between cement and other solid particles are initially filled with water. After setting of fresh concrete, a stiff skeleton is formed and the chemical contraction produced by cement hydration cannot completely transfer to macroscopic shrinkage of concrete. Therefore, with continuation of cement hydration, a number of capillary pores between cement particles are gradually formed and corresponded menisci are created to compensate the volume decrease. Meanwhile, the interior humidity of concrete starts to decrease from the initial saturated state of 100% due to the continuity of liquid water gradually destroyed with the formation of capillary pores. Thus, the development of interior humidity of concrete (RH) at early ages can be described by a vapor saturated stage with 100% relative humidity (stage I) followed by a stage that the relative humidity gradually reduced (stage II). Based on the theory of capillary forces, the shrinkage strain developed in stage I and stage II due to the variation of water content resulted either by cement hydration or by environmental drying may correlate with chemical shrinkage and interior humidity reduction respectively as [4]:

$$\varepsilon = \begin{cases} \eta \left[I - \sqrt[3]{I - (V_{cs} - V_{cs0})} \right] & \text{for } RH = 1 \\ \eta \left[I - \sqrt[3]{I - (V_{cs} - V_{cs0})} \right] + \frac{S V_p \rho R T}{3M} \left(\frac{1}{K_s} - \frac{1}{K} \right) \ln(RH) & \text{for } RH < 1 \end{cases} \quad (1)$$

where η is the influencing factor of stiffness, which is normally a function of water to cement ratio. V_{cs} and V_{cs0} are the chemical shrinkage (in volume) at a given cement hydration degree and at the point where the interior humidity starts to decrease from 100%

¹ Department of Civil Engineering, Key Laboratory of Structural Safety and Durability, China Education Ministry, Tsinghua University, Beijing, 100084, China.

⁺ Corresponding Author: E-mail junz@tsinghua.edu.cn

Note: Submitted January 21, 2013; Revised June 10, 2013; Accepted June 11, 2013.

respectively. M is the molar weight of water (0.01802 kg/mol), ρ is density of water and R is ideal gas constant (8.314 J/molK). K is bulk modulus of the whole porous body and K_s is bulk modulus of the solid material. v_p is obtained by introducing a parameter k_0 in the accumulate pore volume as:

$$v_p = 1 - \exp(-k_0 \beta r) \tag{2}$$

where β is a parameter reflecting the impact of concrete age (reflected by cement hydration degree, α) on pore volume and may be simulated as $\beta = a_0 e^{\lambda \alpha}$, a_0 and λ are experimental determined constants. Parameter k_0 is obtained by comparing model and experimental results [5]. Parameter S in Eq. (1) is called saturation fraction, $S = V_{ew} / V_p$. V_{ew} is the evaporable water content in the hardening cement paste, V_p is the total pore volume. S can be estimated through Powers' volumetric models [6-7]. Assuming the hydration degree of cement is α , and the total volume of cement particles and water is 1, the phase composition of a hardening Portland cement paste without silica fume addition, including chemical shrinkage V_{cs} , capillary pore water volume V_{cw} , gel water volume V_{gw} , gel solid volume V_{gs} and unhydrated cement volume V_c can be calculated through the following equation:

$$\begin{aligned} V_{cs} &= 0.2(1-p)\alpha; V_{cw} = p - 1.3(1-p)\alpha; V_{gw} \\ &= 0.6(1-p)\alpha; V_{gs} = 1.5(1-p)\alpha; V_c = (1-p)(1-\alpha) \end{aligned} \tag{3}$$

where $\sum V_i = 1$, $p = (w/c) / (w/c + \rho_w / \rho_c)$. w and c are the weight of water and cement respectively in concrete mixture. ρ_w and ρ_c are the density of water and cement respectively. So the saturation fraction S can be calculated by:

$$S = \frac{p - 0.7(1-p)\alpha}{p - 0.5(1-p)\alpha} \tag{4}$$

The above equations can be used only for concrete without silica fume application. For the concrete with silica fume addition, the phase composition, including chemical shrinkage V_{cs} , capillary pore water volume V_{cw} , gel water volume V_{gw} , gel solid volume V_{gs} and unhydrated cement particles volume V_c as well as silica fume volume V_s can be estimated by Jensen et al. [7]:

$$\begin{aligned} V_{cs} &= k(0.2 + 0.7s/c)(1-p)\alpha; V_{cw} \\ &= p - k(1.4 + 1.6s/c)(1-p)\alpha; V_{gw} = k(0.6 + 1.6s/c)(1-p)\alpha; \\ V_{gs} &= k(1.6 + 0.7s/c)(1-p)\alpha; V_c = k(1-p)(1-\alpha); V_s \\ &= k(1.4s/c)(1-p)(1-\alpha) \end{aligned} \tag{5}$$

where $\sum V_i = 1$, s , c are the weight of silica fume and cement respectively.

$$p = \frac{w/c}{w/c + \rho_w / \rho_c + (\rho_w / \rho_c)(s/c)}, \quad k = \frac{1}{1 + 1.4(s/c)}$$

Thus, saturation fraction S for concrete with silica fume addition can be calculated by:

$$S = \frac{p - 0.8k(1-p)\alpha}{p - k[0.6 - 0.7(s/c)](1-p)\alpha} \tag{6}$$

The cement hydration degree, α can be calculated from

isothermal tests. By measuring the adiabatic temperature rise of concrete at different time, the cement hydration degree is estimated by:

$$\alpha = \frac{T_{ad}(t)}{T_{ad}(\infty)} \alpha_u \tag{7}$$

where $T_{ad}(t)$ is the adiabatic temperature rising at time t , $T_{ad}(\infty)$ is the ultimate adiabatic temperature rising. α_u is the ultimate degree of hydration and is a function of water to cement ratio (w/c) as [8]:

$$\alpha_u = \frac{1.031w/c}{0.194 + w/c} \tag{8}$$

To calculate the hydration degree under different temperature history, the equivalent age is used. The equivalent age concept assumes that samples of a concrete mixture of the same equivalent age will have the same mechanical properties or cement hydration degree, regardless of the combination of time and temperature yielding the equivalent age. Based on the above definition, the equivalent age t_e can be expressed as

$$t_e = \int_0^t e^{\frac{1}{R} \left(\frac{U_{ar}}{293} - \frac{U_{at}}{273+T} \right)} dt \tag{9}$$

where t_e is the equivalent age at the reference temperature (here the reference temperature is equal to 20°C is assumed). U_{ar} and U_{at} are the apparent activation energy (J/mol) at reference and actual temperature respectively. R is the universal gas constant, 8.314 J/molK. T is temperature in Celsius (°C). Regarding apparent activation energy, a number of researchers have concluded that it could not be considered as a constant independent of time except during the beginning of cement hydration [9-10]. Based on these findings, the apparent activation energy of concrete is expressed as a function of temperature and curing time as [11]:

$$U_a = (42830 - 43T) e^{(-0.00017T)t} \tag{10}$$

where T is curing temperature (°C) and t is curing time in days. Due to the actual temperature T inside of concrete is varied with time, it is convenient to solve t_{eq} in matrix form instead of integrating. If the curing time is divided into n sections and the temperature in each time interval is assumed to be a constant, then we have

$$t_e = \sum_{i=1}^n e^{\frac{1}{R} \left(\frac{U_{ar}}{293} - \frac{U_{aT_i}}{273+T_i} \right)} (t_i - t_{i-1}) \tag{11}$$

The section number n may depend on the required accuracy and normally can be equal to the time intervals for temperature measurement. Based on the equivalent age, the hydration degree of cement defined in Eq. (8) can be simulated by [11-12]:

$$\alpha = \alpha_u \exp\left(-\left(\frac{A}{t_e}\right)^B\right) \tag{12}$$

where A and B are two empirical constants which can be determined by fitting isothermal experimental results and Eq. (13).

Under drying condition, the moisture content in concrete will be less than that under sealed state and this moisture reduction will reduce the cement hydration degree. The effect of moisture content on cement hydration should be taken into consideration in the model by [5]:

$$\frac{d\alpha}{dt_e} = \left(\alpha_c \cdot \frac{B}{A} \left(\ln \left(\frac{\alpha_u}{\alpha} \right) \right)^{\frac{B+1}{B}} - P \right) (RH)^n + P \quad (13)$$

Constants n and P can be determined from interior humidity measurements and isothermal tests. Thus for different drying process, the effect of interior humidity variation on cement hydration can be estimated by Eq. (13). The cement hydration degree at a given time t_e can be obtained by integrating Eq. (13) from 0 to t_e . As showed in Eq. (1), elastic modulus of concrete is also an important parameter for shrinkage calculation. After setting the elastic modulus of concrete starts to grow from zero. Based on the equivalent age, the development of the elastic modulus of concrete with age under varied temperature and drying status can be estimated by [13]:

$$E(\alpha) = 1.05E_{28} \left(\frac{\alpha - \alpha_0}{\alpha_u - \alpha_0} \right)^b \quad (14)$$

where α_0 is the hydration degree at concrete set. b is a constant that can be determined by fitting Eq. (14) with test data. The shrinkage model is based on the formation of capillary pores and resulting capillary stresses during the formation of cement matrix skeleton. Therefore, the model may be used for moisture loss resulted shrinkage prediction regardless if the moisture loss is caused by cement hydration or by environmental drying. Further, by applying present model, the calculation of shrinkage distribution in concrete in the case of humidity gradient existed becomes possible.

The shrinkage model is verified by experiments [5]. Related material parameters used in the model are listed in Table 1. Fig. 1 displays the cement hydration degree and equilibrium age diagrams of the two kinds of concretes with compressive strength at 28 days of 34.1 and 88.7 MPa respectively. Fig. 2 presents the comparisons between model predictions and experimental results for the two kinds of concretes in terms of shrinkage-age diagrams starting from concrete set to 28 days under both sealing and drying curing conditions. From the figure, we can observe that the model can well catch the characteristics of the development of shrinkage of concrete starting from set. Under drying condition, a high shrinkage is obtained in the experiments and in model prediction as well. Because the model combines the effect of age and position into a single physical parameter, RH, the model can predict shrinkage strain in concrete structures not only for discrete time, but also for different positions. Certainly, in order to do so, the moisture distribution, represented by relative humidity inside of concrete is required prior to use the model.

Table 1. Parameters Used in Shrinkage Calculation.

Concrete		C30	C80
η		0.004737	0.04573
Hydration Degree Parameter	α_u	0.8246	0.6261
	A	19.730	17.512
	B	0.6841	0.7980
	α_0	0.2444	0.2910
	α_c	0.5202	0.4899
Elastic Modulus Parameter	$E_{28}(\text{GPa})$	31.0	43.7
	$E_s(\text{GPa})$	72.9	72.9
Pore Structure Parameter	b	0.35	0.99
	k_0	28.25	64.29
Pore Structure Parameter	a_0	0.000673	0.0112
	λ	4.375	2.224

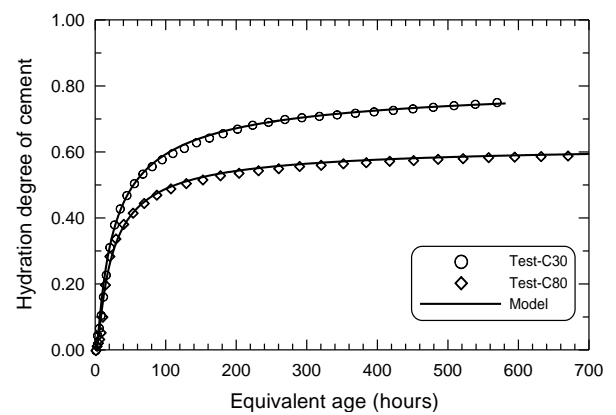


Fig. 1. Relationship of Cement Hydration Degree and Equivalent Age.

Modeling on the Moisture Distribution in Early Age Concrete

The loss of water in early-age concrete is normally caused by both of cement hydration and water diffusion. At the initial period after the concrete cast, most of the pores in concrete are filled by liquid water. The relative humidity in concrete is almost equal to 100%. Due to the process of water consuming is so slow that the period with 100% humidity, which is defined as stage I in the present paper, can last quite long time. When the water content in concrete pores decreases to a critical value, at which the vapor pressure becomes lower than the saturated value, the relative humidity starts to reduce. Starting from this moment, the progress of internal humidity goes into the stage II. Here we may define the length of stage I as the critical time t_c , which is a function of both water to cement ratio and location from casting surface and can be determined by experiments [13]. In the stage II, the variation of water content in terms of relative humidity (RH) is resulted from both cement hydration (RH_s) and water diffusion to environment (RH_d). If one-dimensional water diffusion is considered, according to the second Fick's law, the moisture content balance requires [13]

$$\frac{\partial(H - H_s)}{\partial t} = \frac{\partial}{\partial x} \left(D \frac{\partial(RH - RH_s)}{\partial x} \right) \quad (15)$$

where parameter D is the moisture diffusion coefficient depending

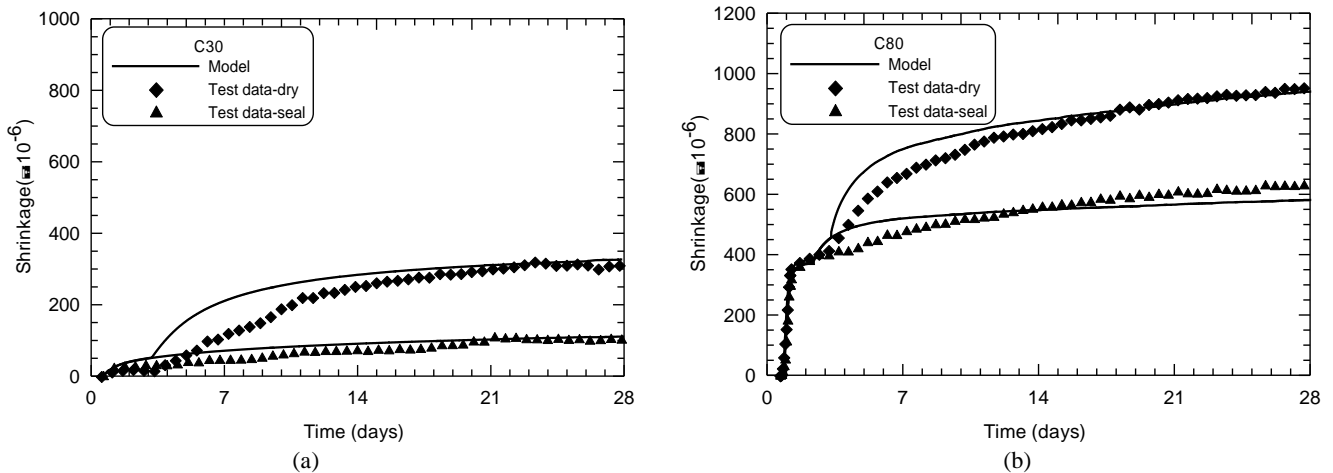


Fig. 2. Comparison between Model and Test Results on Shrinkage of C30 (a) and C80 (b) Concretes.

on the pore humidity and on the composition of concrete [14-17]. Here, RH_s is the humidity reduction due to cement hydration. Let $RH_0 = RH - RH_s$, the above partial differential equation becomes:

$$\frac{\partial RH_0}{\partial t} = \frac{\partial}{\partial x} \left(D \frac{\partial RH_0}{\partial t} \right) \tag{16}$$

For calculating the moisture distribution in concrete exposed to a given atmosphere with an initial condition of 100% relative humidity, Eq. (16) must be solved taking adequate boundary conditions and initial conditions into consideration. However, the relative humidity RH_0 is a function of time (t) and location (x) in concrete and the moisture diffusivity D is also a function of pore humidity. Thus, the distribution of relative humidity along x direction cannot be solved from Eq. (16) directly. In order to overcome this difficulty, we define parameter F as:

$$F = \int_{H_m}^{H_0} D dH_0 \tag{17}$$

Here H_m is a relative humidity that can be selected arbitrarily, normally is equal to the minimum humidity that may occur in concrete. From Eq. (17), we have

$$\frac{\partial F}{\partial H_0} = D, \quad \frac{\partial F}{\partial t} = D \frac{\partial H_0}{\partial t} \tag{18}$$

Using above equations in Eq. (18), we obtain

$$\frac{\partial F}{\partial t} = D \frac{\partial^2 F}{\partial x^2} \tag{19}$$

Thus, the problem for solving H_0 under given time and location becomes solving F from Eq. (21).

Chemical reaction between cement and water can lead to reduction of water content (represented by RH) also. And the magnitude of the humidity reduction resulted from cement hydration must be a function of hydration degree α . In the present work, a modified cement hydration degree based model, which takes the initial liquid-water saturated stage (stage I) into account, is utilized to describe the humidity reduction due to cement hydration

as indicated in Eq. (22).

$$H_s = \begin{cases} 0 & \text{for } \alpha \leq \alpha_c \\ (1 - H_{s,u}) \left(\frac{\alpha - \alpha_c}{\alpha_u - \alpha_c} \right)^\beta & \text{for } \alpha > \alpha_c \end{cases} \tag{20}$$

where $H_{s,u}$ is the relative humidity considering self-desiccation at ultimate degree hydration, which is a function of w/c and can be determined from experiments. α_c is a hydration parameter called critical hydration degree at which the humidity inside of concrete starts to decrease from 100% level, which can be calculated by applying the experimental determined critical time t_c in Eq. (12). The parameter β is a constant.

Using the developed model, we are able to obtain the complete humidity distribution field in early-age concrete. To verify the model, the progress of the humidity inside of concrete is experimentally determined. In the experiments, one dimensional heat and moisture transportation in concrete are made. Waterproof plywood mold with inner dimensions of 200×200×800 mm was used. To allow heat and moisture movement only along the specimen thickness direction, the inner surfaces of the mold were covered with a plastic sheet to prevent moisture loss and the five outer surfaces was covered with polystyrene board to prevent heat loss. Merely the casting face was kept to contact with air directly. In the tests, a digital humidity and temperature combined sensor was used to measure the humidity and temperature. Detailed specimen preparation and test procedures can be found in [13]. Meanwhile, humidity distributions of the concrete slabs are calculated using the developed model. Humidity dependent diffusivity of C30 and C80 concretes used in the model is shown in Fig. 3, which is determined from experiments [17]. The other related parameters used in the model are listed in Table 2. Fig.4 displays comparisons between predicted humidity profiles and test results at some typical ages.

Shrinkage Strain in Concrete Pavement

As an example of application of above models, the distribution of shrinkage strain and stress in concrete pavements made of C30 and C80 concrete respectively is calculated. Assume the slab was cast

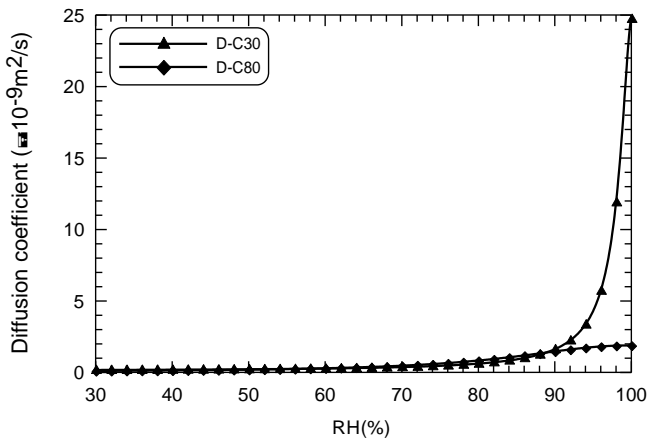


Fig. 3. Water Diffusion Coefficient Used in the Model.

Table 2. Input Parameters Used for Humidity Field Calculation

Concrete	$H_{s,u}$	β	a_m (cm/day)
C30	0.835	3.187	3.0
C80	0.703	1.108	4.1

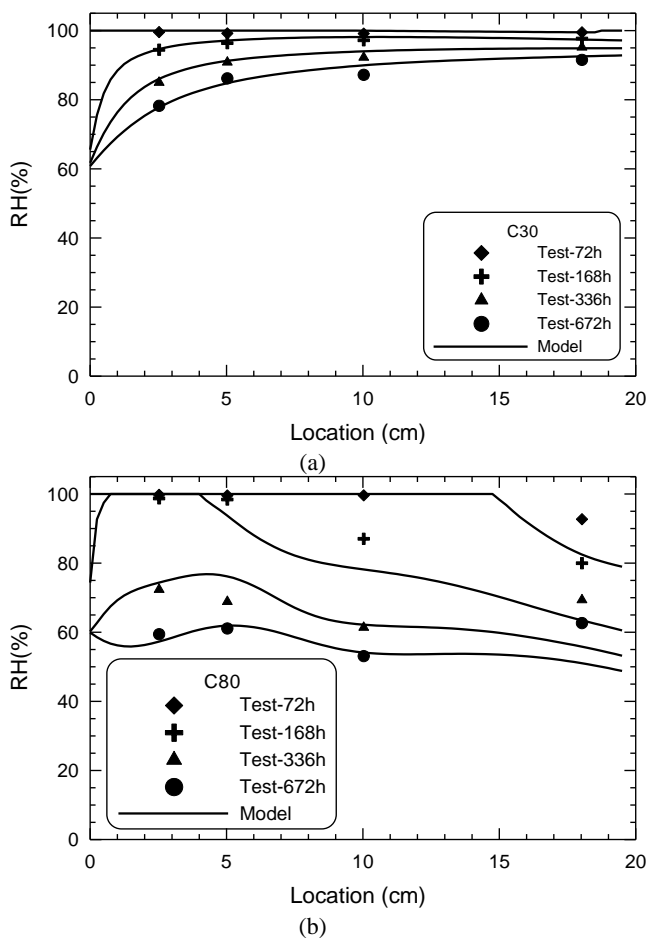


Fig. 4. Comparisons between Predicted Humidity Profile and Experimental Results of C30 (a) and C80 (b) Concrete Slabs.

in spring morning that should influence the development of temperature inside of the slabs. Because the temperature in the slab at early-age is critically needed to calculate the degree of cement

hydration, the development of temperature inside the pavement slab was calculated first in the modeling. After the development of temperature inside of concrete pavement is known, the shrinkage strain and stress induced by cement hydration and environmental drying can then be calculated. Regarding the details of the temperature field calculation may refer to author's previous publication [18].

Fig. 5 presents the model results of the development of interior humidity and corresponding shrinkage strain at different places from top to bottom of the pavements made of C30 and C80 concretes respectively. From the results, first we can observe that the development of interior humidity inside of concrete with age obeys the two stage mode, that is a vapor saturated stage with 100% relative humidity (stage I) and a stage with the relative humidity gradually decreasing (stage II). The humidity gradient along the slab depth is significant and is varied with age. Under the condition that the slab surface undergoes drying, the length of stage I increases with the location from the slab top. Second, the shrinkage strain is well related with interior humidity. Within the stage I, a uniform shrinkage strain is expected throughout the slab. By contrast, the shrinkage gradient along the slab depth is quite obvious in the stage II and the maximum and minimum shrinkages occur at slab top and bottom respectively. That is because the humidity gradient starts to occur in this stage and the maximum and minimum humidity reduction appears at slab top and bottom respectively at the moment. The rate of shrinkage progress is gradually reduced from slab top to bottom in this stage, meaning that the effect of surface drying is confined within a certain range.

The distribution of shrinkage strain along the C30 and C80 concrete slab at some typical ages is displayed in Fig. 6. Clearly, shrinkage distribution along the pavement depth is apparently nonlinear. With development of age, the shrinkage gradient is even pronounced. Concrete strength can significantly influence the magnitude of shrinkage strain as well as its distribution in the slab. At a given age and location, the high the concrete strength, the larger the shrinkage strain and the greater the shrinkage gradient. Here we should note that the shrinkage at slab bottom is close to the magnitude of autogenous shrinkage of concrete and at the slab top surface is a result of a combination of autogenous and drying shrinkage. Apparently, high strength concrete will result in high shrinkage strain as well as high shrinkage gradient in concrete members.

Shrinkage Stress in Concrete Pavement

Decomposing of Nonlinearly Shrinkage Strain

A simple illustration of concrete pavement used in modeling is shown in Fig. 7 and assume the length, width and height of the pavement slab are L , W and H respectively. y is the direction perpendicular to the slab length, x is the direction parallel to the slab length. The long ends of the slab are located at $x = 0$ and $x = L$, respectively. z is the direction parallel to the slab depth and the top and bottom ends of the slab are located at $z = H/2$ and $z = -H/2$, respectively. In the case of the top surface of pavement experiences drying, the variation of shrinkage strain is only obvious through the depth of the slab, the influence of slab width and length can then be

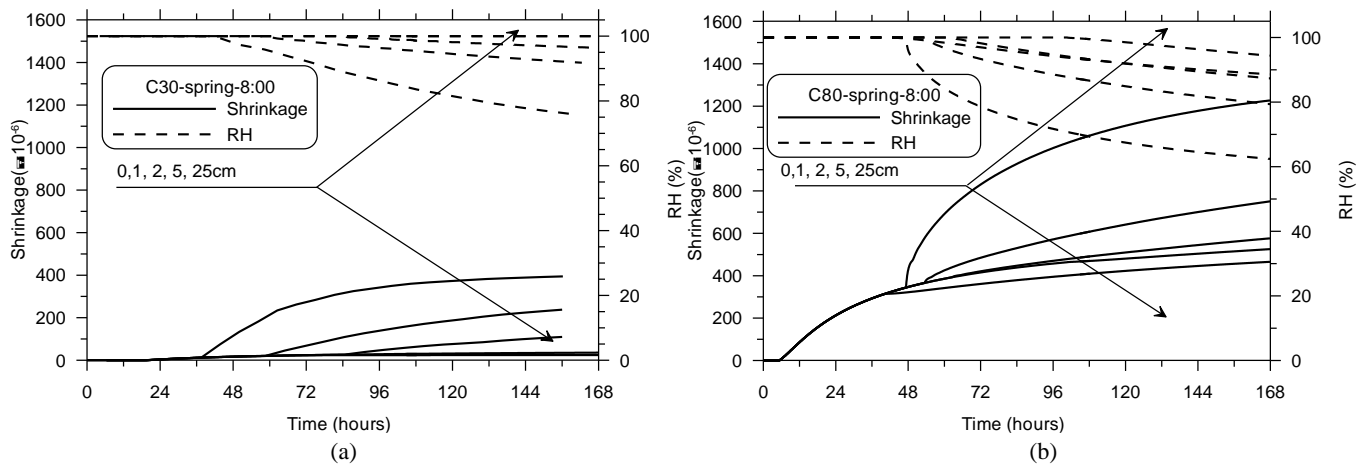


Fig. 5. Development of Shrinkage Strain at Different Locations in Concrete Pavement, (a) C30 and (b) C80.

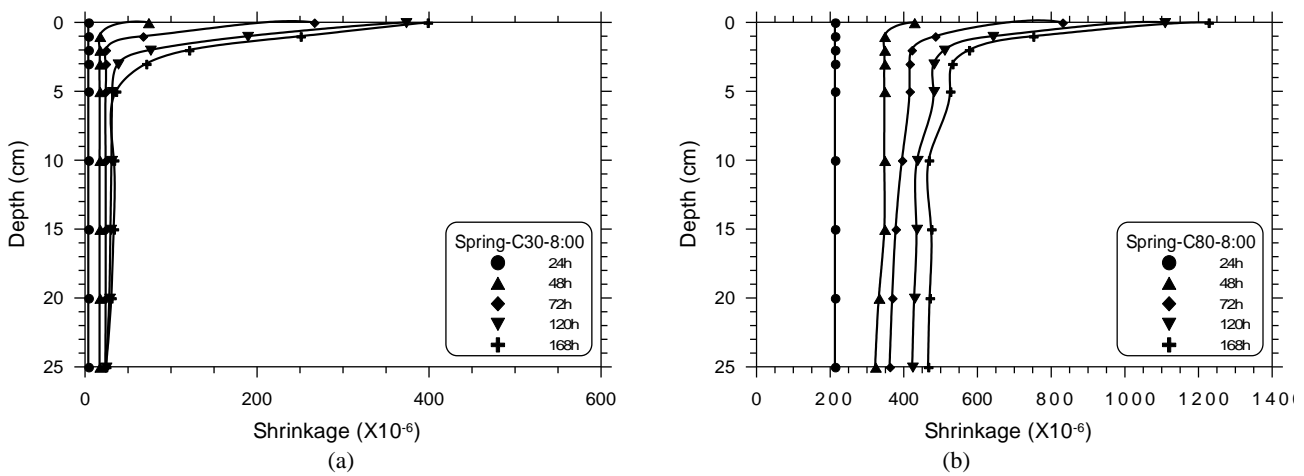


Fig. 6. Distribution of Shrinkage Strain along the Slab Depth at Some Typical Ages, (a) C30 and (b) C80.

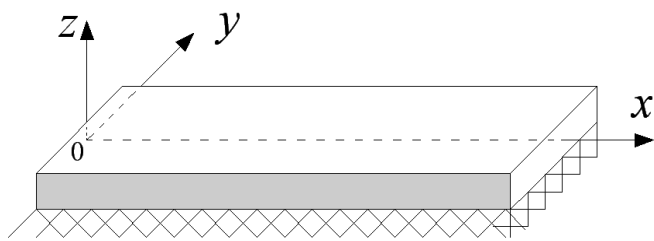


Fig. 7. Schematic Illustration of Concrete Pavement.

neglected. To calculate the stresses resulted from nonlinear distributed shrinkage strain through the depth of the slab, first assume the cross section of the slab remains plane after bending. Thus, the slab can deform only in two ways, expanding or contracting along its axial direction and/or bending with the cross section remaining plane upward or downward. Based on this assumption, under the action of shrinkage stress, the resulted strain distribution through the depth of the slab $\varepsilon(z)$ may be expressed as:

$$\varepsilon(z) = \varepsilon_w - \varepsilon = A + Bz \quad (21)$$

where ε is the nonlinear strain produced in the slab in order to maintain the plane assumption. ε_w is the strain resulted from concrete shrinkage, which is positive and negative respectively as slab expands and shrinks. A and B are constants which can be

obtained from ε_w . The stress produced from ε may be called nonlinear stress, σ_n and can be expressed as:

$$\sigma_n = \frac{E[\varepsilon_w - (A + Bz)]}{1 - \nu} \quad (22)$$

where E and ν are elastic modulus and poisson's ratio of concrete respectively. From the equilibrium conditions of nonlinear stress σ_n [19], we have:

$$A = \frac{1}{H} \int_{-H/2}^{H/2} \varepsilon_w dz = \varepsilon_a \quad (23)$$

$$B = \frac{12}{H^3} \int_{-H/2}^{H/2} \varepsilon_w z dz$$

As long as ε_w is known, the constants A and B can be obtained. Apparently, A is average strain, and B is curvature. Thus, from Eq. (21), the shrinkage strain ε_w can then be expressed as:

$$\varepsilon_w = A + Bz + \varepsilon_n = \varepsilon_a + \varepsilon_l + \varepsilon_n \quad (24)$$

where ε_a , ε_l and ε_n are called average strain, linear strain and nonlinear strain respectively. Thus, the nonlinear shrinkage strain through the depth of the slab can be divided into three components accordingly: 1) a component of uniform shrinkage strain that

principally causes the slab expansion or contraction; 2) a linear component that causes the slab bending; and 3) the nonlinear component that remains after subtracting the uniform and the linear shrinkage strains from the total shrinkage strain.

Shrinkage Stress Resulted from the Uniform Strain Component

To calculate the shrinkage stress produced by the uniform strain component, first assume that the concrete behaves in a linear elastic manner and the base beneath the concrete slab is a rigid material and the deformation under action of the horizontal friction forces is ignored. Second, the resulted average strain in the slab support to simulate stress development along slab length is sufficient to reflect the magnitude of stresses in the slab. This consideration allows the mathematical model to be considered as one-dimensional problem. A concrete pavement section with width W , height H and length L is modeled, see Fig. 7. x is the direction parallel to the slab length and the ends of the slab are located at $x=0$ and $x=L$, respectively. Before derivation of the governing equations for the model, a law governing the slab/base interfacial friction stress-slippage relation is assumed as [20]:

$$\tau = \frac{\tau_0}{\delta_0} |u| \quad \text{for } 0 \leq |u| \leq \delta_0$$

$$\tau = \tau_0 \quad \text{for } |u| > \delta_0$$
(25)

where u is the average slippage along thickness of slab relative to base at location x , given by

$$u(x) = u_c(x) + u_a(x)$$
(26)

where u_c is the displacement induced by concrete shrinkage. u_a is the displacement resulted from internal axial stress. τ_0 is the steady state frictional stress. δ_0 is the corresponding slippage as the frictional stress achieves τ_0 . τ_0 and δ_0 are normally governed by the type of base and they can be determined by sliding tests with a laboratory size slab cast on a given base. When the slab is subjected to a uniform shrinkage strain in the direction of slab length, based on the above assumptions, the axial force equilibrium for a slab length dx in the presence of a thickness average axial stress σ_a and slab/base interfacial shear stress τ requires:

$$\frac{\partial \sigma_a}{\partial x} - \frac{\tau}{H} = 0$$
(27)

The first derivative of σ_c with respect to x can be related to axial displacement u_a by:

$$\frac{\partial \sigma_a}{\partial x} = E \frac{\partial^2 u_a}{\partial^2 x}$$
(28)

Replacing $\frac{\partial \sigma_a}{\partial x}$ with Eq. (30) in Eq. (29) and noting that $\frac{\partial^2 u}{\partial^2 x} = \frac{\partial^2 u_a}{\partial^2 x}$, ($\frac{\partial^2 u_c}{\partial^2 x} = 0$), the general equation governing the average axial displacement distribution in the slab, u is

$$\frac{\partial^2 u}{\partial^2 x} - \frac{\tau}{EH} = 0$$
(29)

According to the magnitude of displacement, the slab may finally be divided into two sections on each of which a specific τ should be applied [19].

Stage I: $|u| \leq \delta_0$ at $x = 0$

In this case, the slab/base interfacial friction stress τ linearly increases with the increase of slab slippage u and this linear friction stress-slippage relationship can be applied along the whole slab. Replacing τ with the linear relation given by Eq. (27) in Eq. (29), we have:

$$\frac{\partial^2 u}{\partial^2 x} - \frac{\tau_0}{EH\delta_0} u = 0$$
(30)

To solve this differential equation with boundary conditions that $u = 0$ at $x = L/2$ and $\partial u / \partial x = \sigma_{a0} / E_c + \varepsilon_a$ at $x = 0$, yields:

$$u = -\frac{1}{\beta} \left[\frac{\sigma_{c0}}{E_c} + \varepsilon_a \right] \frac{\sinh \beta \left(\frac{L}{2} - x \right)}{\cosh \beta \frac{L}{2}}$$
(31)

where $\beta = \sqrt{\tau_0 / EH\delta_0}$ and σ_{a0} is average axial stress at $x = 0$ along slab thickness. Here, we define σ_{a0} as negative if it compresses the slab and positive if it tensions the slab. Similarly, if ε_a is negative, the shrinkage makes the slab shorter and if it is positive, it makes the slab longer. The sign of u is governed by the combined effect of ε_a and σ_{a0} . Positive u means that the slab becomes shorter and a negative value means that the slab becomes longer. From Eq. (28), the stress σ_a can be expressed as

$$\sigma_a = E \left[\frac{\partial u}{\partial x} - \varepsilon_a \right]$$
(32)

Substitution of u with Eq. (33) into Eq. (34) gives:

$$\sigma_a = -E\varepsilon_a \left[1 - \frac{\cosh \beta \left(\frac{L}{2} - x \right)}{\cosh \beta \frac{L}{2}} \right] + \sigma_{a0} \frac{\cosh \beta \left(\frac{L}{2} - x \right)}{\cosh \beta \frac{L}{2}}$$
(33)

Stage II: $|u| > \delta_0$ at $x = 0$

In this case, the slab should be divided into two sections according to the displacement relative to base. Now assume $u = \delta_0$ at $x = x_0$, for the section of $0 \leq x \leq x_0$, the slab/base interfacial friction stress is fully developed and the shear stress is a constant. Replace τ with τ_0 in Eq. (31), the general governing equation of u can be rewritten as

$$\frac{\partial^2 u}{\partial^2 x} - \frac{\tau_0}{EH} = 0$$
(34)

To solve this differential equation with boundary conditions that $\partial u / \partial x = \sigma_{a0} / E_c + \varepsilon_a$ at $x = 0$ and $u = \delta_0$ at $x = x_0$, yields:

$$u = \delta_0 + \frac{1}{2} \beta^2 \delta_0 (x^2 - x_0^2) + \left[\frac{\sigma_{a0}}{E_c} + \varepsilon_a \right] (x - x_0) \tag{35}$$

Similar to stage I, using Eq. (37) in Eq. (34), the stress in slab within this location can be expressed as

$$\sigma_a = E\beta^2 \delta_0 x + \sigma_{a0} \tag{36}$$

For the section of $x_0 < x \leq L/2$, the slab/base frictional stress is being developed due to the small slab slippage ($u \leq \delta_0$). The procedures used to solve the average displacement and stress fields in stage I can be applied in this section by simply replacing the slab length $L/2$ with $(L/2 - x_0)$ and using a new boundary condition at $x = x_0$ instead of at $x = 0$, i.e. $\partial u / \partial x = \sigma_{a00} / E_c + \varepsilon_a$ at $x = x_0$. σ_{a00} is the thickness average axial stress at $x = x_0$. The displacement and stress fields in this section are given by

$$u = -\frac{l}{\beta} \left[\frac{\sigma_{a00}}{E} + \varepsilon_a \right] \frac{\sinh \beta \left(\frac{L}{2} - x \right)}{\cosh \beta \left(\frac{L}{2} - x_0 \right)} \tag{37}$$

and

$$\sigma_a = -E\varepsilon_a \left[1 - \frac{\cosh \beta \left(\frac{L}{2} - x \right)}{\cosh \beta \left(\frac{L}{2} - x_0 \right)} \right] + \sigma_{a00} \frac{\cosh \beta \left(\frac{L}{2} - x \right)}{\cosh \beta \left(\frac{L}{2} - x_0 \right)} \tag{38}$$

where $\sigma_{a00} = E_c \beta^2 \delta_0 x_0 + \sigma_{a0}$. The length x_0 can be numerically determined from Eq. (19) by setting $x = x_0$ and $u = \delta_0$. It should be noted that σ_{a0} may be related to crack bridging law of concrete in general if the slab ends are associated with crack location. The present work is focused on analyzing the development of shrinkage stress in jointed concrete pavements at early-age, so that $\sigma_{a0} = 0$ is used in the examples of analyses.

Shrinkage Stress Resulted from the Linear Strain Component

The general solution for an elastic slab subjected to linear strain profile was given as

$$\begin{aligned} -\frac{\partial^2 w}{\partial x^2} &= \frac{12}{Eh^3} (M_x - \nu M_y) + B \\ -\frac{\partial^2 w}{\partial y^2} &= \frac{12}{Eh^3} (M_y - \nu M_x) + B \end{aligned} \tag{39}$$

where x, y, z are the directions of slab length, width and thickness respectively. w is the displacement in the z -direction. The right side of the above equation represents the total curvature of the slab corresponding to the moment curvature in x and y direction and the curvature due to the linear strain gradient respectively. The stresses

produced by the linear strain difference can be obtained by solving above differential equations with appropriate boundary and external restrained conditions. In the present work, research is focus on the solving of shrinkage stresses in concrete pavement in early-age. The slab is normally relatively long and the restraint action along the slab length is significant. So we may assume that $\partial^2 w / \partial x^2 = 0$. Thus from Eq. (39), we have

$$\begin{aligned} M_y &= \frac{Eh^3}{12(1-\nu)} \left[-\frac{\partial^2 w}{\partial x^2} - (1+\nu)B \right] \\ M_x &= \nu M_y - \frac{Eh^3}{12} B \end{aligned} \tag{40}$$

In addition, the moment M_y can be related to the reacting force of base kw by

$$\frac{d^2 M_y}{dy^2} = kw \tag{41}$$

where k is the stiffness of the pavement base. Replace M_y with Eq. (40) in Eq. (41), the general governing equation of w can be rewritten as

$$l^4 \frac{\partial^4 w}{\partial y^4} + w = 0 \tag{42}$$

where $l = \left[\frac{Eh^3}{12(1-\nu^2)k} \right]^{1/4}$. Solve the above differential equation with boundary conditions that $M_y = 0$ and $dM_y/dy = 0$ at $y = \pm W/2$ yields:

$$\begin{aligned} w = w_0 & \frac{2 \cos W_l \cosh W_l}{\sin 2W_l + \sinh 2W_l} \left[(-tg W_l + \tanh W_l) \cos \frac{y}{l\sqrt{2}} \cosh \frac{y}{l\sqrt{2}} \right. \\ & \left. + (tg W_l + \tanh W_l) \sin \frac{y}{l\sqrt{2}} \sinh \frac{y}{l\sqrt{2}} \right] \end{aligned} \tag{43}$$

here $w_0 = (1+\nu)Bl^2$, $W_l = W/(l\sqrt{8})$. Thus replace w in Eq. (43) with Eq. (44), we can obtain the expression of the stress distribution in x and y direction through the depth of the slab as

$$\begin{aligned} \sigma_{yz} &= 2\sigma_0 \left\{ 1 - \frac{2 \cos W_l \cosh W_l}{\sin 2W_l + \sinh 2W_l} \left[(tg W_l + \tanh W_l) \cos \frac{y}{l\sqrt{2}} \cosh \frac{y}{l\sqrt{2}} \right. \right. \\ & \left. \left. + (tg W_l - \tanh W_l) \sin \frac{y}{l\sqrt{2}} \sinh \frac{y}{l\sqrt{2}} \right] \right\} \frac{z}{H} \\ \sigma_{xz} &= 2 \left[\sigma_0 + \nu (\sigma_{yz} - \sigma_0) \right] \frac{z}{H} \end{aligned} \tag{44}$$

where $\sigma_0 = EBH / 2(1-\nu)$, which is the stress as slab length and width are infinite and the deformation produced by the shrinkage differences is fully restrained. The maximum stress produced by the linear shrinkage component will occur at the section with $y = 0$ in the direction of x -axial. The stress distribution in the section of $y = 0$ along x -direction, σ_{xz} can be expressed as

$$\sigma_{xz} = 2\sigma_0 [1 - \nu(1 - C_y)] \frac{z}{H} \tag{45}$$

where $C_y = 1 - \frac{2 \cos W_l \cosh W_l}{\sin 2W_l + \sinh 2W_l} (tg W_l + \tanh W_l)$, that is a function of slab width and depth as well as stiffness of slab and the supporting base.

Shrinkage Stress Resulted from the Nonlinear Component

According to the assumption that the cross section of the pavement remains plane under the action of shrinkage strain, the stress caused by the nonlinear component can be calculated by

$$\sigma_n = -\frac{E}{1-\nu} (\epsilon_w - A - Bz) \tag{46}$$

Thus, the total shrinkage stresses produced by such nonlinear shrinkage strain in the slab can be obtained by summing the three stress components together as:

$$\sigma_i = \sigma_a + \sigma_l + \sigma_n \tag{47}$$

Creep Correction on the Shrinkage Stresses

Creep of concrete leads to the stress relaxation. To correctly calculate the shrinkage stresses in concrete pavement, the effect of concrete creep must be taken into account. In the present paper, a method given by Zhu [19] is used to correct the effect of concrete creep. Assume the initial stress without considering of the effect of creep at time t_0 is equal to σ_0 . After the time period $(t-t_0)$, the stress becomes $\sigma(t)$ due to the action of creep. Now assume the time interval $(t-t_0)$ is divided into n sections, $\Delta t_1, \Delta t_2, \Delta t_3, \dots, \Delta t_i, \dots, \Delta t_n$, and the stress increment in each time section is $\Delta \sigma_1, \Delta \sigma_2, \Delta \sigma_3, \dots, \Delta \sigma_i, \dots, \Delta \sigma_n$. Thus the stress at time t can then be given as:

$$\sigma(t) = \sigma(t_0) + \sum_{i=1}^n \Delta \sigma_i(t_i) \tag{48}$$

where $t_i = t_0 + \sum_{i=1}^{n-i} \Delta t_i$. As taking the concrete creep into account, the stress with an initial value of $\sigma(t_0)$ after the time period $(t-t_0)$ can be calculated by:

$$\sigma(t, t_0) = \sigma(t_0) \left[1 - \frac{\varphi(t, t_0)}{1 + \varphi(t, t_0)} \right] \tag{49}$$

where $\varphi(t, t_0)$ is called creep coefficient and can be calculated by Bazant et al [21]:

$$\varphi(t, t_0) = \varphi_1 t_0^{-d} (t - t_0)^p \tag{50}$$

where φ_1, d and p are material parameters. In present paper, $\varphi_1 = 0.9, d = 0.32, p = 0.32$ are used in the model calculation according to the reference [21]. Thus, the shrinkage stresses as considering the effect of concrete creep can be given as:

Table 3. Frictional Restraint Characteristics of Typical Base.

Base Type	τ_0 (MPa)	δ_0 (mm)	k (GPa)
Cement Stabilized	0.106	0.025	81

$$\sigma(t, t_i) = \sigma(t_0) \left[1 - \frac{\varphi(t, t_0)}{1 + \varphi(t, t_0)} \right] + \sum_{i=1}^n \Delta \sigma(t_i) \left[1 - \frac{\varphi(t, t_i)}{1 + \varphi(t, t_i)} \right] \tag{51}$$

Analyses of Shrinkage Stress in Concrete Pavement at Early-Ages

As an example of the model application, the shrinkage stress in concrete pavements made of C30 and C80 concrete respectively is calculated. The cement stabilized base is assumed and the friction restraint parameters between slab and base as well as the stiffness of base used in the model are list in Table 3. For modeling, it is assumed that the dimension of the slab is 10 meters in length, 4 meters in width and 0.25 meters in thickness. The shrinkage stress calculation is based on above prediction of shrinkage strain (ϵ_w).

Fig. 8(a) shows the development of the total shrinkage stress in the middle section of C30 concrete slab with age, where the effects of location from top to bottom are displayed. Fig. 8(b) shows the development of the total shrinkage stress at slab top with age, where the effect of location in length direction is presented. Fig. 9 show analogous results of C80 concrete pavement. From these results, we can see that shrinkage stress occurred in concrete pavement under the condition that the slab top experiences drying are function of construction age, location in both length and depth directions. First, for given age and surface drying condition, the shrinkage stress increases with location in length direction and the maximum stress achieve at the center of the slab. Such behavior is the result of interfacial friction between slab and supporting base occurred during concrete shrinking. Therefore, the variation of shrinkage stress with location in length direction is only controlled by the average shrinkage strain component, A , which in turn is governed by the overall shrinkage distribution in the slab and its variation with age as well. Second, for given age and length location, the variation of shrinkage stress along slab depth is principally controlled by the shrinkage gradient. The linear and nonlinear strain components are the main contributor to such stress variation through the depth. Third, shrinkage stresses along the pavement depth is nonlinearly distributed. The stress gradient is more and more pronounced with time going. Fourth, concrete strength can significantly influence the magnitude of shrinkage stress, as well as its distribution in the slab. At a given age and location, the higher the concrete strength, the larger the shrinkage stress and the greater the stress gradient. In addition, we may be noted also from Fig. 9 that the influencing scope of surface drying on the shrinkage stress is a function of concrete strength and age. Influencing depth increases with age for all three kinds of concretes. In the view of durability design of concrete structures, all above characteristics related to shrinkage stress occurred in concrete members should considerably be taken into account.

Conclusions

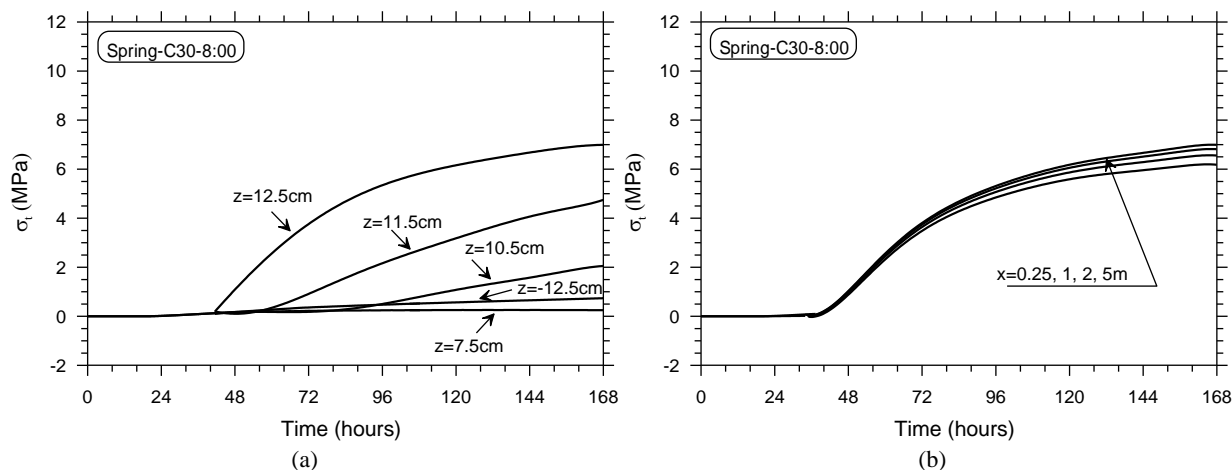


Fig. 8. Development of Shrinkage Stress in C30 Concrete Pavement, (a) Showing the Effect of Location in Depth and (b) Showing the Effect of Location in Length.

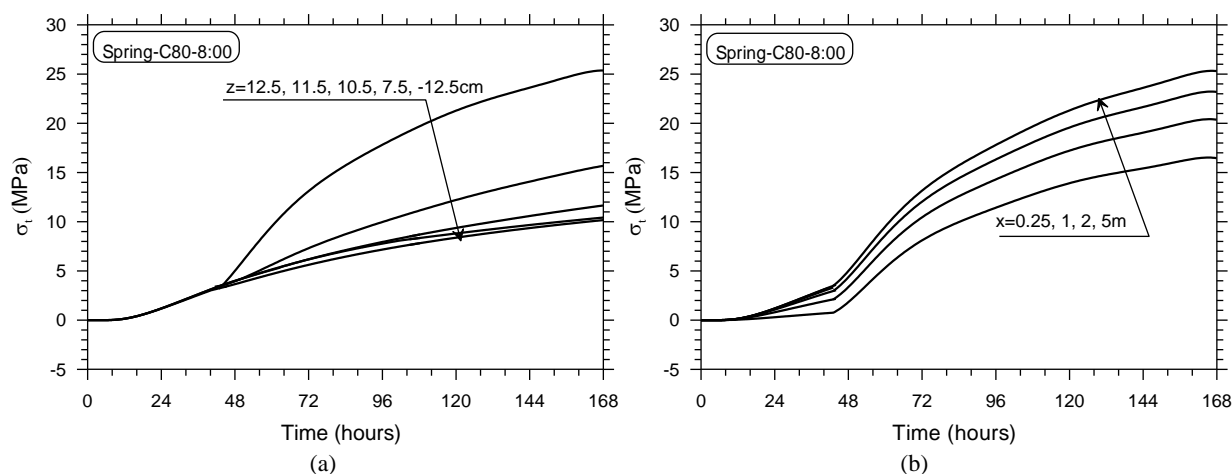


Fig. 9. Development of Shrinkage Stress in C80 Concrete Pavement with Consideration of Creep, (a) Showing the Effect of Location in Depth and (b) Showing the Effect of Location in Length.

In this paper, an integrative model for shrinkage strain and stress in concrete pavements at early-age from concrete cast are simulated and analyzed. The model results show that the progress of internal humidity inside of pavement since concrete cast obeys two stage mode, that is a vapor saturated stage with 100% relative humidity (stage I) and a stage with the relative humidity gradually decreasing (stage II). Within stage I, a uniform shrinkage strain and stress is expected throughout the slab. By contrast, shrinkage gradient along the slab depth is quite significant in stage II and the maximum and minimum shrinkage strain and stress occur at slab top and bottom respectively. The distribution of shrinkage strain and stress along the pavement depth is nonlinear and the nonlinearity is strong close to the drying area. Concrete strength can significantly influence the magnitude of shrinkage strain and stress, as well as their distribution in the slab.

Acknowledgements

This work has been supported by grants from the National Science Foundation of China (No. 50978143, 51178248) to Tsinghua University.

References

1. Ayano, T., Wittmann, F.H. (2002). Drying, Moisture Distribution, and Shrinkage of Cement-based Materials. *Materials and Structures*, 35(247), pp.134-140.
2. Bissonnette B, Pierre P, Pigeon M. (1999). Influence of Key Parameters on Drying Shrinkage of Cementitious Materials. *Cement and Concrete Research*, 29(10), pp. 1655-1662.
3. Zhang, J., Hou, D. W. and Sun, W. (2010). Experimental Study on the Relationship Between Shrinkage and Interior Humidity of Concrete at Early Age. *Magazine of Concrete Research*, 62(3) pp. 191-199.
4. Zhang, J., Hou, D. and Chen, H. (2011). Experimental and Theoretical Studies on Shrinkage of Concrete at Early-ages. *ASCE Journal of Materials in Civil Engineering*, 23(3), pp. 312-320.
5. Zhang, J., Hou, D. and Han Y. (2011). Micromechanical Model of Autogenous and Drying Shrinkages of Concrete. *Building and Construction Materials*, 29(3), pp. 230-240.
6. Powers, T.C. and Brownyard, T.L. (1946). Studies of the Physical Properties of Hardened Portland Cement Paste. *Journal of America Concrete Institute*. 43, Bulletin 22,

- Research Laboratories of the Portland Cement Association, Chicago.
7. Jensen, O.M. and Hansen, P.F. (2001). Water-entrained Cement-based Materials: I. Principles and Theoretical Background. *Cement and Concrete Research*, 31(5), pp. 647-654.
 8. Rastrup, E. (1954). Heat of Hydration. *Magazine of Concrete Research*, 6(17), pp. 127-140.
 9. Kjellsen, K. and Detwiler, R.J. (1993). Later-age Strength Prediction by a Modified Maturity Model. *ACI Materials Journal*, 90(3), pp. 220-227.
 10. Chanvillard, G. and Daloia, L. (1997). Concrete Strength Estimation at Early Age: Modification of the Method of Equivalent Age. *ACI Materials Journal*, 94(6), pp. 220-227.
 11. Kim, J.K. (2001). Estimation of Compressive Strength by a New Apparent Activation Energy Function. *Cement and Concrete Research*, 31(2), pp. 217-225.
 12. Pane, I. and Hansen, W. (2002). Concrete Hydration and Mechanical Properties under Nonisothermal Conditions. *ACI Materials Journal*, 99(6), pp. 534-422.
 13. Zhang, J., Qi, K. and Huang, Y. (2009). Calculation of Moisture Distribution in Early-age Concrete. *ASCE Journal of Engineering Mechanics*, 135(8), pp. 871-880.
 14. Akita, H., Fujiwara, T. and Ozaka, Y. (1997). A practical procedure for the analysis of moisture transfer within concrete due to drying. *Magazine of Concrete Research*, 49(179), pp. 129-137.
 15. Bazant, Z.P., and Najjar, L.J. (1972). Nonlinear Water Diffusion in Nonsaturated Concrete. *Materials and Structures*, 5(25), pp. 3-20.
 16. Nilsson, L.O. (2002). Long-term Moisture Transport in High Performance Concrete. *Materials and Structures*, 35, pp. 641-649.
 17. Zhang, J., Hou, D. Gao Y. and Sun, W. (2011). Determination of Moisture Diffusion Coefficient of Concrete at Early-age from Interior Humidity Measurements. *Drying Technology*, 29(6), pp. 689-696.
 18. Hou, D. Zhang, J. and Gao, Y. (2012). Simulation of temperature field of concrete pavement at early age. *Engineering Mechanics*, 29(6), pp.151-159 (in Chinese).
 19. Zhu, B.F. (1999). *Thermal Stress and Temperature Control in Mass Concrete*. Electric Power Publishing House, Beijing, China (in Chinese).
 20. Zhang, J. and Li, V.C. (2001). Influence of Supporting Base Characteristics on the Shrinkage Induced Stresses in Concrete Pavements. *ASCE Journal of Transportation Engineering*, 127(6), pp. 455-462.
 21. Bazant, Z.P. and Panula, L. (1978). Practical Prediction of Time Dependent Deformation of Concrete. *Materials and Structures*, Part I and II, 11(65), pp. 307-328; parts III and IV, 11(66), pp.415-434; Parts V and VI, 12(69), pp. 169-173.